AFRL-AFOSR-VA-TR-2019-0165

In Vivo Probing of Quantum Coherence in Bacterial Photosynthesis

Jennifer Ogilvie
REGENTS OF THE UNIVERSITY OF MICHIGAN

05/21/2019
Final Report

Air Force Research Laboratory
AF Office Of Scientific Research (AFOSR)/ RTB2
Arlington, Virginia 22203
Air Force Materiel Command

REPORT DOCUMENTATION PAGE

Form Approved
OMB No. 0704-0188

1. REPORT DATE *(DD-MM-YYYY)*	2. REPORT TYPE	3. DATES COVERED *(From - To)*
21-06-2019	Final Performance	15 Feb 2018 to 14 Feb 2019

4. TITLE AND SUBTITLE
In Vivo Probing of Quantum Coherence in Bacterial Photosynthesis

5a. CONTRACT NUMBER

5b. GRANT NUMBER
FA9550-18-1-0124

5c. PROGRAM ELEMENT NUMBER
61102F

6. AUTHOR(S)
Jennifer Ogilvie

5d. PROJECT NUMBER

5e. TASK NUMBER

5f. WORK UNIT NUMBER

7. PERFORMING ORGANIZATION NAME(S) AND ADDRESS(ES)
REGENTS OF THE UNIVERSITY OF MICHIGAN
503 THOMPSON ST
ANN ARBOR, MI 48109-1340 US

8. PERFORMING ORGANIZATION REPORT NUMBER

9. SPONSORING/MONITORING AGENCY NAME(S) AND ADDRESS(ES)
AF Office of Scientific Research
875 N. Randolph St. Room 3112
Arlington, VA 22203

10. SPONSOR/MONITOR'S ACRONYM(S)
AFRL/AFOSR RTB2

11. SPONSOR/MONITOR'S REPORT NUMBER(S)
AFRL-AFOSR-VA-TR-2019-0165

12. DISTRIBUTION/AVAILABILITY STATEMENT
A DISTRIBUTION UNLIMITED: PB Public Release

13. SUPPLEMENTARY NOTES

14. ABSTRACT

This project aimed to employ the first spatially-resolved multidimensional spectroscopy to enable the elucidation of quantum effects in biological systems. Using purple sulfur photosynthetic bacteria as a model system, we aimed to understand the physical origin of recently observed quantum coherence in photosynthetic antennae complexes and to determine its importance for efficient energy transfer. In our previous AFOSR-funded work we developed fluorescence-based multidimensional spectroscopies to enable extensive characterization of coherent dynamics in isolated photosynthetic complexes and in vivo in purple bacterial cells. Here we used the approach to demonstrate that the method can resolve growth-dependent changes in the excitonic structure of purple bacteria in vivo1. We also performed theoretical work to model the fluorescence-detected two dimensional electronic spectroscopy (F-2DES) data from these systems2. In addition we have observed coherence in the LH2 complex of purple bacteria and have extensively characterized it3. We find that the coherence is largely electronic in nature, with a rapid ~30 fs dephasing time, making it unlikely that it plays a role in energy transfer processes which occur on a ~picosecond timescale. Our measurements pose a challenge to theoretical and computational approaches to capture the observed quantum and non-equilibrium phenomena. With an understanding of the key design elements of biological systems that exploit quantum effects to optimize their function, it may be possible to mimic such design principles in artificial materials for energy capture, conversion and human use. The proposed research supports technological advances in application areas of interest to the United States Air Force, including bio-molecular and atomic imaging below the diffraction limit, biologically inspired new innovative and novel materials, human perfo

15. SUBJECT TERMS
quantum, coherence, spectroscopy

16. SECURITY CLASSIFICATION OF:			17. LIMITATION OF ABSTRACT	18. NUMBER OF PAGES	19a. NAME OF RESPONSIBLE PERSON
a. REPORT	b. ABSTRACT	c. THIS PAGE			BIN-SALAMON, SOFI
Unclassified	Unclassified	Unclassified	UU		19b. TELEPHONE NUMBER *(Include area code)* 703-696-8411

Final report: *In Vivo* Probing of Quantum Coherence in Bacterial Photosynthesis

This project aimed to employ the first spatially-resolved multidimensional spectroscopy to enable the elucidation of quantum effects in biological systems. Using purple sulfur photosynthetic bacteria as a model system, we aimed to understand the physical origin of recently observed quantum coherence in photosynthetic antennae complexes and to determine its importance for efficient energy transfer. In our previous AFOSR-funded work we developed fluorescence-based multidimensional spectroscopies to enable extensive characterization of coherent dynamics in isolated photosynthetic complexes and *in vivo* in purple bacterial cells. Here we used the approach to demonstrate that the method can resolve growth-dependent changes in the excitonic structure of purple bacteria *in vivo*[1]. We also performed theoretical work to model the fluorescence-detected two dimensional electronic spectroscopy (F-2DES) data from these systems[2]. In addition we have observed coherence in the LH2 complex of purple bacteria and have extensively characterized it[3]. We find that the coherence is largely electronic in nature, with a rapid ~30 fs dephasing time, making it unlikely that it plays a role in energy transfer processes which occur on a ~picosecond timescale. Our measurements pose a challenge to theoretical and computational approaches to capture the observed quantum and non-equilibrium phenomena. With an understanding of the key design elements of biological systems that exploit quantum effects to optimize their function, it may be possible to mimic such design principles in artificial materials for energy capture, conversion and human use. The proposed research supports technological advances in application areas of interest to the United States Air Force, including bio-molecular and atomic imaging below the diffraction limit, biologically inspired new innovative and novel materials, human performance and enhanced computational development for future Air force needs.

1) First spatially resolved detection of the excitonic structure and ultrafast processes in purple bacterial membranes[1]

By combining our F-2DES approach with confocal microscopy we demonstrated a sensitive new imaging approach capable of mapping spatially-varying differences in electronic couplings using a correlated map of excitation and detection frequencies, with sensitivity orders of magnitude better than conventional spatially-averaged electronic spectroscopies. The approach performs fluorescence-detection-based fully collinear two-dimensional electronic spectroscopy in a microscope, combining femtosecond time-resolution, sub-micron spatial resolution, and the sensitivity of fluorescence detection (see Fig. 1). We demonstrate the approach on a mixture of photosynthetic bacteria that are known to exhibit variations in electronic structure with growth conditions. Spatial variations in the constitution of mixed bacterial colonies manifests as spatially-varying peak intensities in the measured two-dimensional contour maps, which exhibit well-resolved electronic couplings between excited electronic states of the bacterial proteins.

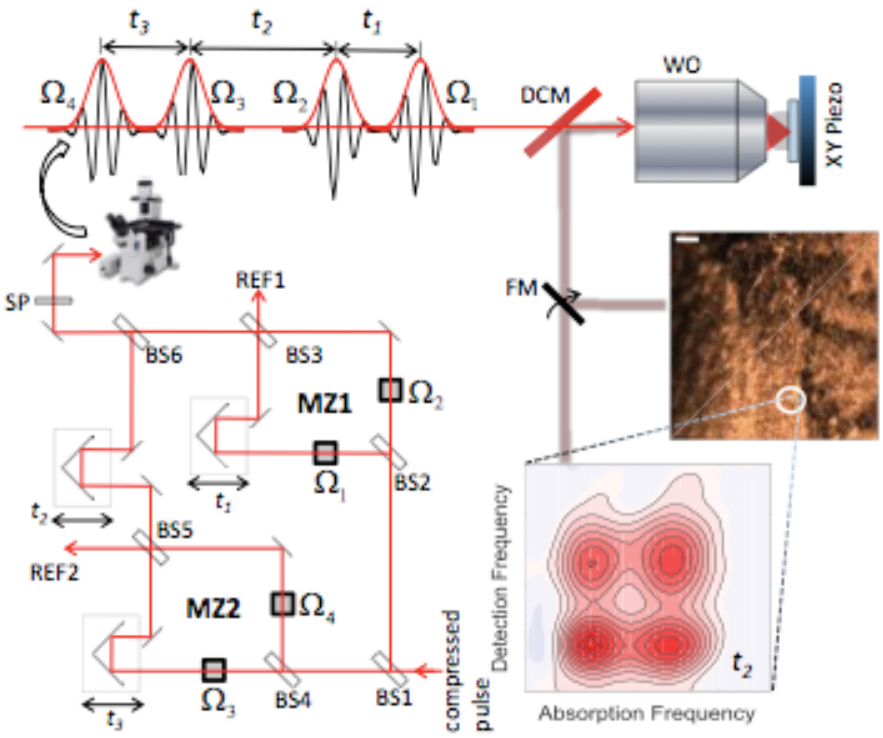

Fig. 1. A simplified description of the spatially-resolved F- 2DES spectrometer (SF 2DES). A given pulse in the compressed laser pulse train is split 50:50 by a beam-splitter (BS1), and each half is routed into a Mach-Zehnder (MZ) interferometer (MZ1 and MZ2). Each of the four interferometer arms (two per MZ) contains an AOM which sweeps the carrier-envelope phase of the pulse by frequency Ω_i, i = 1 − 4. The time intervals between the four pulses, t_1, t_2 and t_3 are controlled by mechanical delay stages. One output port from each MZ is used to generate a reference signal REF1(2) which is utilized by the lock-in amplifier for signal detection. The other output port from each MZ is combined at BS6, generating four collinear time separated pulses (pump and probe pulse pairs), which are optically filtered by a shortpass filter (SP), and routed into a confocal microscope. A dichroic mirror (DCM) in the microscope transmits the collinear pulse train towards a water objective (WO), which focuses it on an immobilized sample. The sample is mounted on an XY scanning piezo stage (PZ). The fluorescence collected by the WO is separated from the excitation light at the DCM, and can be either routed for fluorescence imaging, or for generating a 2D map. An example of the fluorescence image, and the 2D spectrum at a desired XY location is shown in the figure. The 2D spectrum corresponds to zero waiting time between pump and probe pulse pairs ($t_2 = 0$), and shows absorptive changes in the refractive index of the sample in the form of well-resolved 2D peakshapes. Cross peaks at t2 = 0 indicate that the absorption and detection frequencies of the system are different. This implies that the transitions corresponding to the positions of the two diagonal peaks correspond to excitonic transitions between sites which are electronically coupled on the excited state, and therefore connected via a common ground state.

Fig. 2 shows *in vivo* measurements illustrating how the growth condition dependent perturbation of the electronic structure of purple bacteria manifests in the SF -DES spectra. Fig. 2a shows fluorescence images collected from a bacterial colony in unmixed samples of LL (upper panel) and HL (lower panel) bacteria. Multiple XY locations on these fluorescence maps were chosen to collect fluorescence detected 2DES spectra. Fig. 2b shows the averaged absorptive fluorescence detected 2DES

spectra for LL and HL bacteria. The positions of the two diagonal peaks correspond to the B800 (upper diagonal) and B850 (lower diagonal) excitonic manifolds of the LH2 antennae within the bacterial cells. The effect of growth conditions on spectral properties is reflected by the varying strength of the lower (B850) diagonal peak. This is better seen in Fig. 2d, which compares slices through the maxima of the diagonal peaks for the LL and HL cases. The measurements show that between HL and LL conditions, the 2D diagonal peak strengths change by a factor of four, that is, the ratio of B850/B800 diagonal peak changes from 2:1 to 1:2. The measured changes are well above the error bars of the measurement, emphasizing that the SF 2DES spectrometer is able to distinguish between the two kinds of cells with a respectable signal-to-noise ratio. Higher error bars near the peak slopes in Fig. 2d reflect the fact that any index shifts in the 2D spectra, resulting from trial-to-trial variations, are averaged over.

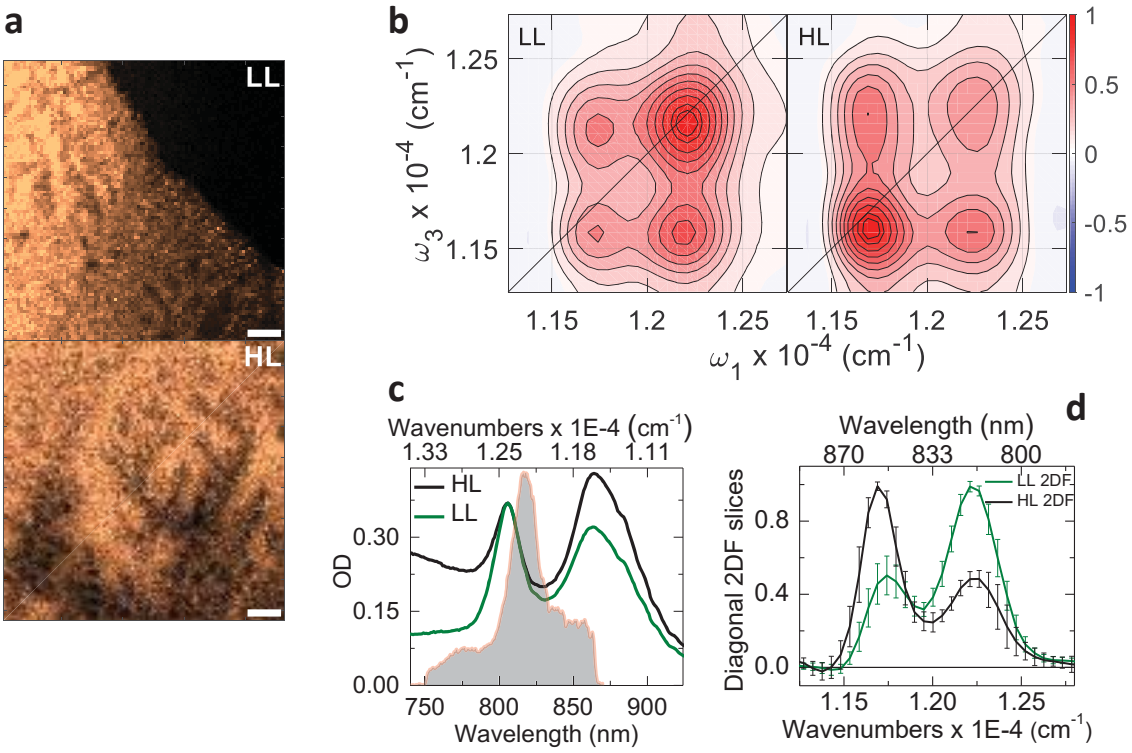

Fig. 2. SF-2DES on unmixed cells of Rps. palustris grown under high-light (HL) and low-light (LL) light intensity conditions. (a) Confocal fluorescence images of a drop-dried film of photosynthetic bacteria Rps. palustris. The bacteria were grown under LL (top panel), and HL (bottom panel) conditions. A 10 μm scale bar is shown for reference. The OD of the live cell solution from which the samples were prepared is shown in panel c, and the drop volume was measured to be ~0.08 μl through gravimetric analysis (SI). (b) Normalized absorptive 2D spectra at t2 = 0 fs obtained by averaging 2D spectra from 5 different XY locations on the LL and HL fluorescence images, as shown in the left and right panels respectively. The spectra show well-resolved cross-peaks at t2 = 0 fs. Contours are drawn at 10-90 % in steps of 10%, 95% and 100%. The frequency ω corresponding to the axes labels on the 2D plots corresponds to ω =| ω′ | /2πc, where ω′ is in rad/fs.(c) Linear absorption spectrum for LL and HL grown Rps. palustris overlaid with the laser spectrum (grey area). The OD for the LL sample is scaled by a factor of 0.37 such both samples have the same OD at the B800 band. (d) Slices through the

maxima of the upper and lower diagonal peaks of the LL and HL 2D spectra shown in panel b. The error bars are obtained from averaging LL and HL 2D spectra at 5 different locations on the fluorescence images of panel a. The solid black line across the 2D plot corresponds to the diagonal. All measurements were conducted at 300 K.

The background-free nature of fluorescence-detection, coupled with the development of high quantum efficiency single-photon detectors has made single molecule fluorescence detection routine. Thus, in terms of scalability of 2DES to very low numbers of absorbers, fluorescence-detection approach may hold more promise than heterodyne-detection of a radiated electric field, as typically employed in ensemble 2DES experiments. Our experiments demonstrate that F-2DES is highly sensitive: for experiments in which the sample was recirculated, a respectable signal-to-noise ratio was attainable with ODs ~ 5x lower (in a 200 μm pathlength) than those used in previous in vivo studies, with the estimated probed volume ~ 6 orders of magnitude smaller due to the FWM PSF created by the microscope objective.

We have demonstrated *in vivo* spatially-resolved measurements of 2D electronic spectra from colonies of photosynthetic bacteria grown under different light intensity conditions and have resolved the resulting differences in excitonic structure of the antenna proteins inside the cells. The Coulomb couplings between electronic levels and their perturbations with growth conditions are reflected as spatial variations in the well-resolved 2D peak amplitudes that arise from spatial heterogeneity in the bacterial colonies. The fluorescence-detection approach we adopt offers significant sensitivity improvements over conventional heterodyne detection. Employing phase-modulation rather than phase-cycling enables imaging at high repetition rates, and produces spectra with a high signal-to-noise ratio without the need to combine multiple phase-cycled scans that could be susceptible to photobleaching. This work serves as a demonstration of the broad applicability of the SF-2DES approach towards resolving the connections between morphological variations, the resulting electronic couplings, and ultimately the performance of a variety of light-harvesting materials.

2) Fluorescence-detected Two-Dimensional Electronic Spectroscopy of Multichromophoric Systems – Application to Understanding the Excitonic Structure of LH2[2]

Working in collaboration with the group of Thomas La Cour Jansen, we developed a theory for modeling fluorescence-detected two-dimensional electronic spectroscopy (F-2DES) of multichromophoric systems[2]. We tested the theory via comparison of the predicted spectra of the light-harvesting complex LH2 with our experimental data, allowing us to gain insight into the stark differences between our F-2DES data and previous studies of LH2 using the more conventional coherent-detected 2DES approach. This allowed us to explain the

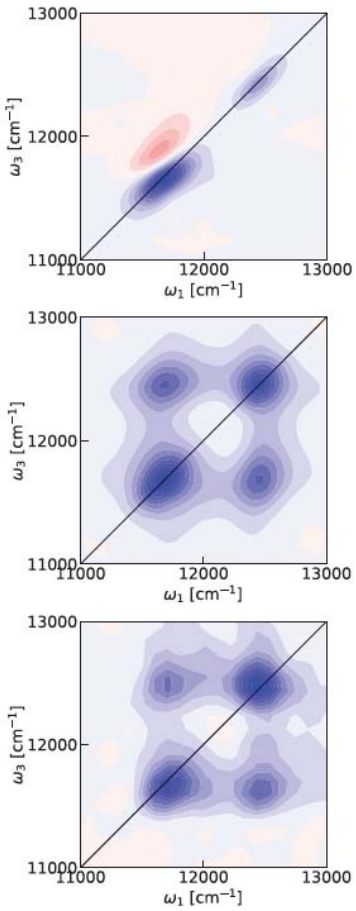

Fig. 3 2DES spectra of LH2 at T = 0 fs with parallel polarization. Blue color indicates bleach signal, whereas red color indicates induced absorption. The contours change color for every 10% of the maximum intensity in the individual plot. Top: Simulated 2DES spectrum. Middle: Simulated F-2DES. Bottom: Experimental F-2DES spectrum.

presence of strong cross-peaks in the F-2DES data that are absent in 2DES. Fig. 3 shows simulated F-2DES and 2DES spectra, as well as our F-2DES data for LH2, demonstrating that our simulations capture the main features of the F-2DES data nicely. Previous work by the La Cour Jansen group has shown good agreement with 2DES measurements[4]. Fig. 4 shows a decomposition of the different signal components of the F-2DES and 2DES spectra as predicted by the theory. The sum of these different components yields the spectra shown in Fig. 3. Within the theory we attribute the strong presence of cross-peaks in the F-2DES data to the clean ground-state signal that is revealed when the annihilation of exciton pairs created on the same LH2 complex cancels oppositely signed signals from the doubly excited state. This annihilation process occurs much faster than the nonradiative relaxation. Furthermore, the line shape difference is attributed to slow dynamics, exciton delocalization within the bands, and intraband exciton−exciton annihilation. This is in line with existing theories presented for model systems. In contrast, the 2DES spectra do not exhibit strong cross-peaks, due to the opposite sign of excited state absorption (ESA) and ground state bleach (GSB) and stimulated emission (SE) signals. This demonstrates the strong potential for F-2DES to detect weak coupling that is obscured in 2DES measurements.

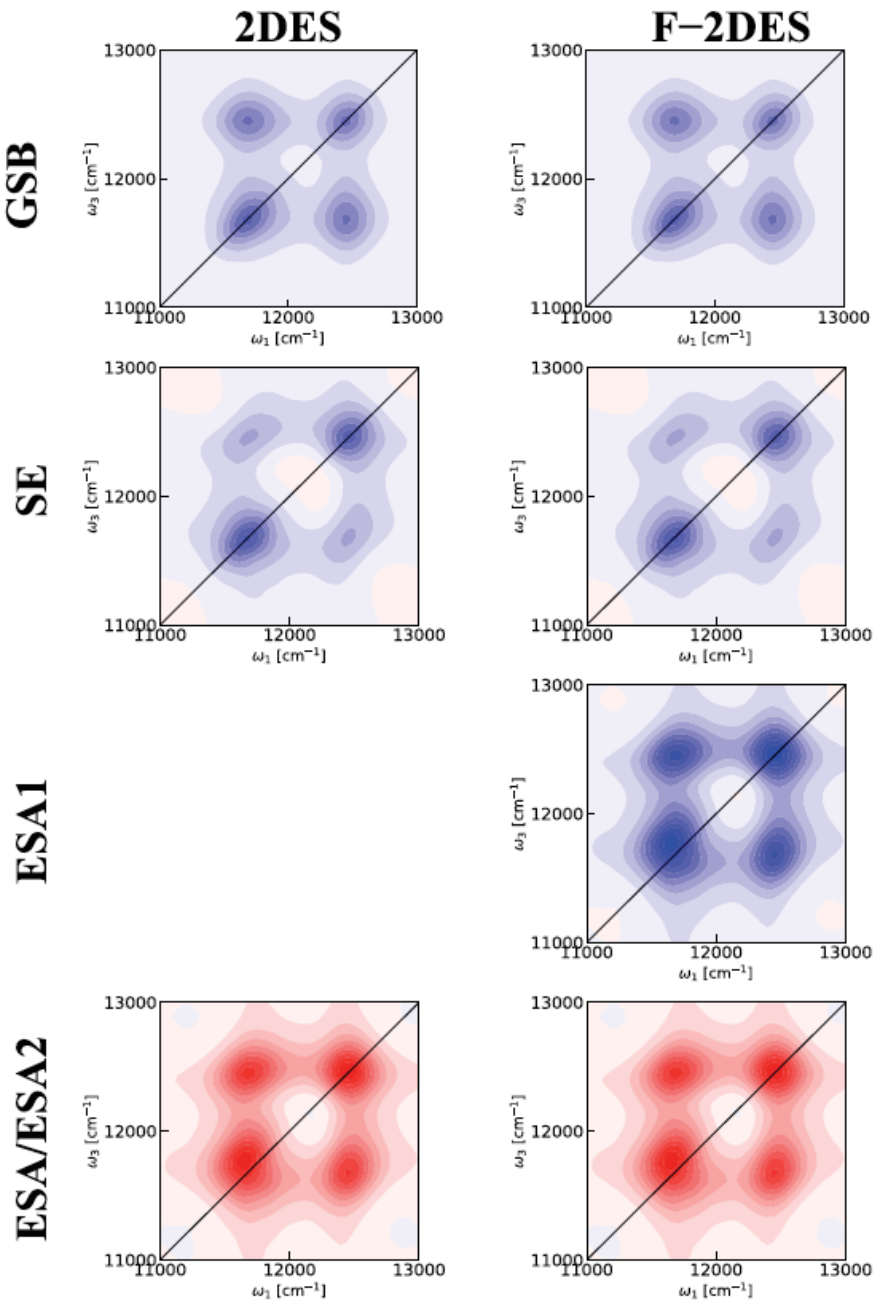

Fig. 4 Components contributing to the 2DES spectra of LH2 at T = 0 fs with parallel polarization. Blue color indicates bleach signal, whereas red color indicates induced absorption. The contours change color for every 10% of the maximum intensity of the ESA contributions. For 2DES spectra, the GSB, SE, and ESA signals contribute equally. For F-2DES spectra, the ESA1 and the ESA2 signal contributions are equal in magnitude but opposite in sign, leading to a cancellation of the ESA signals and clear observation of the positive cross-peaks in the F-2DES spectra.

3) Understanding the Nature of Coherence in LH2 *in vivo*[3]

There has been considerable ongoing debate about the physical origin of coherence in photosynthetic systems and its possible relevance to the photosynthetic functions of energy transfer and charge separation[5]. Previous studies of the LH2 complex have reported the observation of coherence but have differed in their interpretation of its physical origin; whether the coherence was electronic, vibrational, or mixed vibronic. We previously demonstrated that our F-2DES approach is highly sensitive to coherent dynamics in a model dimer system[6]. It is known that in *R. Palustris*, the excitonic structure of LH2 is altered when cells are grown under high light (HL) vs low light (LL) conditions, such that the B850-B800 energy gap LH2 from LL cells is reduced by ~100 cm^{-1}. Since the frequency of electronic coherence matches the frequency gap between the two participating electronic states, a careful comparison of coherence frequency can be used to verify the possible electronic nature of the coherence. We performed F-2DES studies on HL and LL whole cells and isolated LH2 from HL and LL cells and carefully characterized their coherence frequencies and dephasing times. Fig. 5 shows representative data depicting coherence at cross-peak (CP) and diagonal peak (DP) positions in the rephrasing and nonrephasing F-2DES spectra at locations where electronic coherence is expected. Also shown are global fits to a damped exponential for the data for the HL (red) and LL (blue) cases. The coherence frequencies extracted from the HL and LL cells display a frequency difference of 88 ± 15 cm^{-1}, which supports their assignment as electronic interband B800-B850 coherence. Further support of this assignment comes from the rapid dephasing time of 30 ± 5 fs. In contrast, vibrational coherence is expected to diphase on picosecond timescales, and should not change frequency in HL and LL cells which contain the same bacteriochlorophyll pigments with the same vibrational modes. We are currently writing up our results for publication[3]. Given the rapid 30 fs dephasing time of the coherence, we believe that it is unlikely to be important for energy transfer between B800 and B850 rings, which is known to occur on a picosecond timescale. However, it is possible that the dephasing time we have measured is artificially shortened due to ensemble averaging. We are pursuing studies on smaller numbers of complexes, approaching the single molecule level, to test this hypothesis.

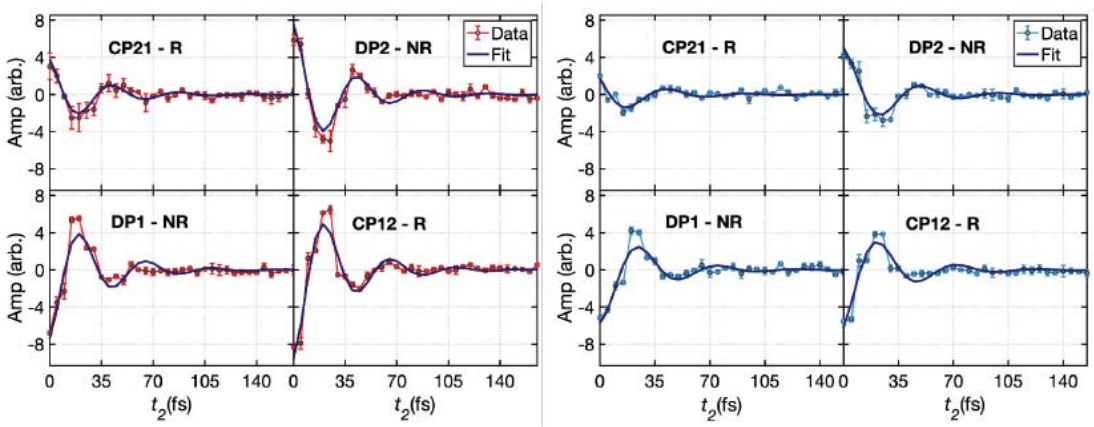

Fig. 5 Two-color F-2DES *T* time traces extracted from HL (red) and LL (blue) isolated Rps. palustris LH2 complexes in solution. For each cell type the four different pulse sequences described in Figure 5.4 were employed for selective excitation of coherences appearing at CP12 and CP21 (rephasing) and DP1 and DP2 (nonrephasing). Time traces shown from 0 to 165 fs in 5 fs steps along *T* for HL and 0 to 155 fs in 5 fs steps

for LL. Three data sets were collected from each pulse sequence experiment and all twelve runs were performed consecutively for each cell type. The time traces are averaged over three trials with error bars showing the standard error of the mean. Averaged traces from each region were globally fit to one damped sinusoidal oscillation (dark blue) for HL and LL independently.

1. Tiwari, V.; Acosta Matutes, Y.; Gardiner, A.; Cogdell, R. J.; Ogilvie, J. P. *Nature Communications* **2018,** 9, 4219.
2. Kunsel, T.; Tiwari, V.; Matutes, Y. A.; Gardiner, A. T.; Cogdell, R. J.; Ogilvie, J. P.; Jansen, T. L. C. *The Journal of Physical Chemistry B* **2019,** 123, (2), 394-406.
3. Acosta Matutes, Y.; Tiwari, V.; Gardiner, A.; Cogdell, R. J.; Ogilvie, J. P. *in preparation* **2019**.
4. van der Vegte, C. P.; Prajapati, J. D.; Kleinekathoefer, U.; Knoester, J.; Jansen, T. L. C. *Journal of Physical Chemistry B* **2015,** 119, (4), 1302-1313.
5. Cao, J.; Cogdell, R. J.; Coker, D. F.; Duan, H.-G.; Hauer, J. r.; Kleinekathöfer, U.; Jansen, T. L. C.; Mančal, T.; Miller, R. J. D.; Ogilvie, J. P.; Prokhorenko, V. I.; Renger, T.; Tan, H.-S.; Tempelaar, R.; Thorwart, M.; Thyrhaug, E.; Westenhoff, S.; Zigmantas, D. *submitted* **2019**.
6. Tiwari, V.; Acosta Matutes, Y.; Yu, Z.; Ptaszek, M.; Bocian, D. F.; Holten, D.; Kirmaier, C.; Konar, A.; Ogilvie, J. P. *Optics Express* **2018,** 26, (17), 22327-22341.